View Article Online
View Journal

PAPER

Understanding the structural complexity of dissolved organic matter: isomeric diversity†

Dennys Leyva, [ID] [ab] Lilian V. Tose,[a] Jacob Porter,[a] Jeremy Wolff,[c] Rudolf Jaffé[b] and Francisco Fernandez-Lima [ID] *[ad]

In the present work, the advantages of ESI-TIMS-FT-ICR MS to address the isomeric content of dissolved organic matter are studied. While the MS spectra allowed the observation of a high number of peaks (*e.g.*, PAN-L: 5004 and PAN-S: 4660), over 4× features were observed in the IMS-MS domain (*e.g.*, PAN-L: 22 015 and PAN-S: 20 954). Assuming a total general formula of $C_xH_yN_{0-3}O_{0-19}S_{0-1}$, 3066 and 2830 chemical assignments were made in a single infusion experiment for PAN-L and PAN-S, respectively. Most of the identified chemical compounds (∼80%) corresponded to highly conjugated oxygen compounds (O_1–O_{20}). ESI-TIMS-FT-ICR MS provided a lower estimate of the number of structural and conformational isomers (*e.g.*, an average of 6–10 isomers per chemical formula were observed). Moreover, ESI-q-FT-ICR MS/MS at the level of nominal mass (*i.e.*, 1 Da isolation) allowed for further estimation of the number of isomers based on unique fragmentation patterns and core fragments; the later suggested that multiple structural isomers could have very closely related CCS. These studies demonstrate the need for ultrahigh resolution TIMS mobility scan functions (*e.g.*, $R = 200$–500) in addition to tandem MS/MS isolation strategies.

Introduction

Dissolved organic matter (DOM) is a highly complex mixture of organic compounds that is ubiquitous in aquatic ecosystems, resulting mainly from the degradation of aquatic and terrestrial primary producers.[1] It is mainly composed of carbon, hydrogen and oxygen, with the other elements being at relatively lower abundance. The biogeochemical functions of natural DOM are extremely important because of their influence on many environmental processes, including the fate and transport

[a]*Department of Chemistry and Biochemistry, Florida International University, Miami, FL 33199, USA. E-mail: fernandf@fiu.edu*

[b]*Southeast Environmental Research Center, Florida International University, Miami, Florida 33199, USA*

[c]*Bruker Daltonics, Inc., Billerica, Massachusetts 01821, USA*

[d]*Biomolecular Sciences Institute, Florida International University, Miami, FL 33199, USA*

of contaminants, ecological processes and water treatment.[1] Despite the important role of DOM in global carbon cycling, and while tens of thousands of molecular formulas have been reported in DOM,[2,3] and many structural features identified,[4] the molecular structures of most components in this complex mixture remain largely unknown.[5] This is primarily due to the fact that DOM components are highly variable in volatility, polarity, molecular structure, functionality and elemental composition, leading to serious challenges in their separation and identification.[3] However, the combination of multiple analytical approaches[2,6] and the utilization of advanced analytical techniques have moved this field forward. In particular, Fourier Transform Ion Cyclotron Resonance Mass Spectrometry (FT-ICR MS) and Quadrupole Time-of-Flight Mass Spectrometry (Q-TOF-MS) have aided much in the characterization of DOM due to their high resolution capabilities and flexibility toward coupling with separation techniques. While FT-ICR MS has been widely and successfully used to assess the molecular composition of DOM, limitations with regards to isomer characterization, an important aspect of DOM complexity, still remain. A recent report focused on characterizing DOM complexity and composition in a highly variable set of DOM samples using FT-ICR MS in combination with advanced statistical methods,[7] confirmed the notion that a significant component of DOM seems to be molecularly indistinguishable between samples and is thus ubiquitous in the environment.[8] Not only the co-occurrence of thousands of identical molecular formulae, but also, a remarkable similarity of fragment ion intensities among samples, and thus molecular structure commonalities, were reported.[7] Using a modeling approach, the authors estimated the isomers associated with the large number of identified molecular formulas. However, constraining isomerization aspects in DOM characterization continues to be challenging, and such information might be most accurately achieved by Ion Mobility Spectrometry (IMS) in tandem with mass spectrometry.[9]

During the last few decades, several attempts have been made to utilize IMS in tandem with mass spectrometry for the analysis of complex mixtures.[9] A common trend is towards the possibility to separate chemical classes by their IMS-MS trend lines, measurement of ion-neutral collision cross sections, shorter analysis time, easy coupling to other separation techniques (*e.g.*, gas and liquid chromatography), increased peak capacity and reduction of the chemical noise. With the advent of high resolution mobility analyzers ($R > 80$), there is a natural push for their integration with high resolution mass analyzers for the analysis of complex mixtures.[10–19] Our team pioneered the integration of trapped IMS (TIMS) with FT-ICR MS in 2015,[20] and several reports have shown the unique advantages of TIMS-FT-ICR MS.[9,21–27]

In the present work, we discuss the advantages and current challenges during ESI-TIMS-FT-ICR MS/MS analysis of complex mixtures. The goal is to address the analytical advantages of ESI-TIMS-FT-ICR MS and ESI-q-FT-ICR MS/MS for two freshwater DOM samples in assessing their isomeric diversity and future challenges provided from MS/MS experiments at nominal mass.

Experimental

Sample preparation

Surface water was collected from Pantanal (PAN) National Park – SE Brazil, one of the largest subtropical and biodiverse freshwater wetlands in the world. The PAN

samples were collected from the Paraguay River (PAN-L) and a wetland channel in Pantanal National Park (PAN-S). For further details on sampling and sample preparation, see ref. 2. The DOM and the individual standards were dissolved in 50 : 50 v/v methanol/water to a final concentration of 1 ppm. Prior to analysis, all samples were spiked with 5% (v/v) of the Tuning Mix calibration standard. All solvents used were of Optima LC-MS grade or better, obtained from Fisher Scientific (Pittsburgh, PA).

Sample ionization

An electrospray ionization (ESI) source based on the Apollo II ESI design (Bruker Daltonics, Inc., MA) was used in negative ion mode for all experiments. Sample solutions were introduced into the nebulizer at a rate of 360 μL h^{-1} using a syringe pump. Typical operating conditions were 3000–3500 V capillary voltage, 10 L min^{-1} dry gas flow rate, 1.0 bar nebulizer gas pressure, and a dry gas temperature of 180 °C.

Trapped ion mobility spectrometry analysis

The concept behind TIMS is the use of an electric field to hold ions stationary against a moving gas, so that the drag force is compensated by the electric field and ion packages are separated across the TIMS analyzer axis based on their mobility.[28–30] During mobility separation, a quadrupolar field confines the ions in the radial direction to increase trapping efficiency. The mobility, K, of an ion in a TIMS cell is described by:

$$K = \frac{v_g}{E} \cong \frac{A}{(V_{elution} - V_{out})} \tag{1}$$

where v_g, E, $V_{elution}$ and V_{out} are the velocity of the gas, applied electric field, elution voltage and tunnel out voltage, respectively. Mobility spectra were calibrated using a Tuning Mix calibration standard (Tunemix, G2421A, Agilent Technologies, Santa Clara, CA) with the following reduced mobility (K_0) values: m/z 301 $K_0 = 1.909$, m/z 601 $K_0 = 1.187$, m/z 1033 $K_0 = 0.776$, and m/z 1333 $K_0 = 0.710$ cm^2 V^{-1} s^{-1}.[31,32]

The mobility values (K) can be correlated with the ion-neutral collision cross section (Ω, Å^2) using the Mason–Schamp equation:

$$\Omega = \frac{(18\pi)^{1/2}}{16} \frac{z}{(k_B T)^{1/2}} \left(\frac{1}{m_I} + \frac{1}{m_b}\right)^{1/2} \frac{1}{K} \frac{760}{P} \frac{T}{273.15} \frac{1}{N^*} \tag{2}$$

where z is the charge of the ion, k_B is the Boltzmann constant, N^* is the number density, and m_I and m_b refer to the masses of the ion and bath gas, respectively.[33]

ESI-TIMS-FT-ICR MS/MS analysis

All experiments were performed on a custom built ESI-TIMS-q-FT-ICR MS 7T Solarix spectrometer equipped with an infinity ICR cell (Bruker Daltonics Inc., MA). The TIMS analyzer is controlled using in-house software, written in National Instruments Lab VIEW, and synchronized with the 7T Solarix FT-ICR MS acquisition program. TIMS separation was performed using nitrogen as a bath gas at ca. 300 K, $P_1 = 2.2$ and $P_2 = 0.9$ mbar, and a constant rf (2200 kHz and 140–160

Vpp). A nonlinear stepping scan function was used,[27] with a gate width of 3 ms. The TIMS cell was operated using a fill/trap/elute/quench sequence 9/3/9/3 ms, using an average of 1000 IMS scans per MS spectrum and a voltage difference across the ΔE gradient of 5.0 V. The ramp voltage gradient was stepped by 0.25 V per frame with a ΔV_{ramp} range of -160 to -60, for a total of 400 steps. The deflector (V_{def}), funnel entrance (V_{fun}), analyzer base (V_{out}) and gating lens (V_{gate}) voltages were $V_{def} = -180/180$ V, $V_{fun} = -90$ V, $V_{out} = -50$ V and $V_{gate} = -80$ V/ 80 V. TIMS-FT-ICR MS spectra were processed using sine-squared apodization followed by Fast Fourier Transform (FFT), in magnitude mode, resulting in an experimental MS resolving power of $R \sim 400\,000$ at m/z 400. ESI-q-FT-ICR MS/MS experiments were performed using quadrupole isolation at nominal mass and typical CID energies of 15–20 eV.

Data processing

The ESI-TIMS-FT-ICR MS spectra were externally calibrated for mass and mobility using the Agilent ESI-L mass calibration standard. The formulae calculations from the exact mass domain were performed using Composer software (Version 1.0.6, Sierra Analytics, CA) and confirmed with Data Analysis (Bruker Daltonics v 4.2) using formula limits of $C_x H_y N_{0-3} O_{0-19} S_{0-1}$, and odd and even electron configurations were allowed. The TIMS spectrum for each molecular formula was processed using a custom-built Software Assisted Molecular Elucidation (SAME) package – a specifically designed 2D TIMS-MS data processing script written in Python v2.7.[34] SAME package utilizes noise removal, mean gap filling, "asymmetric least squares smoothing" base line correction, peak detection by continuous wavelet transform (CWT)-based peak detection algorithm (SciPy package), and Gaussian fitting with non-linear least squares functions (Levenberg–Marquardt algorithm). The SAME final outcome is [m/z; chemical formula; K; collision cross section (CCS)] for each TIMS-MS dataset. The 2D TIMS-MS contour plots were generated in Data Analysis (Version v. 5.1, Bruker Daltonics, CA) and all the other plots were generated using matplotlib and OriginPro 2016 (Originlab Co., MA). The MetFrag CL software was used for *in silico* determination of potential candidate structures using the PubChem database.[35]

Results and discussion

ESI-TIMS-FT-ICR MS analysis

The analysis of the PAN complex dissolved organic matter using ESI-TIMS-FT-ICR MS resulted in a single, broad trend line in the IMS-MS domain composed of singly charged species (Fig. 1). Inspection of the MS domain leads to the observation of a similar profile of a single, broad Gaussian distribution centered around m/z 400, regardless of the sample.

Closer inspection of the MS spectra allowed a comparison of the number of MS peaks (*e.g.*, PAN-L: 5004 and PAN-S: 4660), with the number of IMS-MS features (*e.g.*, PAN-L: 22 015 and PAN-S: 20 954). Assuming a total general formula of $C_x H_y N_{0-3} O_{0-19} S_{0-1}$, we found 3066 and 2830 for PAN-L and PAN-S compounds, respectively. Most of the identified chemical compounds (~80%) corresponded to highly conjugated oxygen compounds (O_1–O_{20}), in good agreement with previous
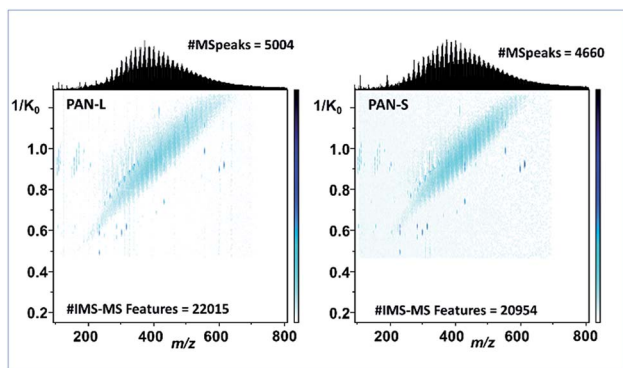
Fig. 1 Typical 2D-IMS-MS contour plots for the cases of the PAN-L and PAN-S complex dissolved organic matter.

reports.[36] This complexity can be visualized at the level of nominal mass (see example in Fig. 2) for 391 m/z.

ESI-q-FT-ICR MS/MS analysis

While a large isomeric diversity is observed at the level of nominal mass and per chemical formula, complementary information on the nature of the sample constituents can be obtained by performing ESI-q-FT-ICR MS/MS. At the level of nominal mass, several m/z signals are observed (*e.g.*, over 7 at 391 m/z). When subjected to Collision Induced Dissociation (CID), several common neutral losses are observed (see Fig. 3 and Tables S1–S3†).

If we assume that the neutral losses can be directly associated with functional groups and the overall structure of the parent ion, a number of potential structural isomers can be estimated for a given chemical formula; under this assumption, conformational isomers will present the same fragmentation
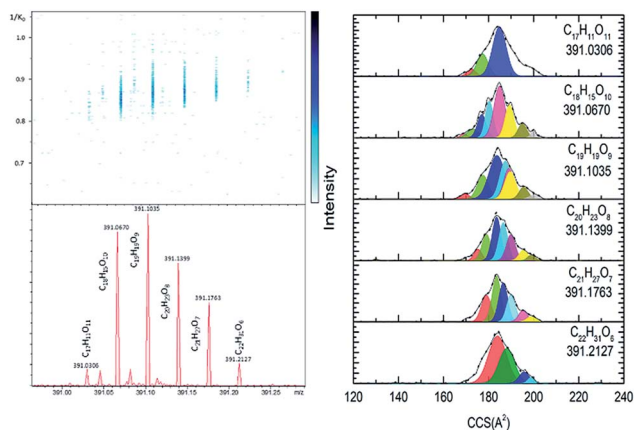

Fig. 2 Typical 2D-IMS-MS, as well the MS and IMS projections at nominal mass (*i.e.*, 391 m/z). Different bands are annotated in the IMS projections based on the SAME algorithm.
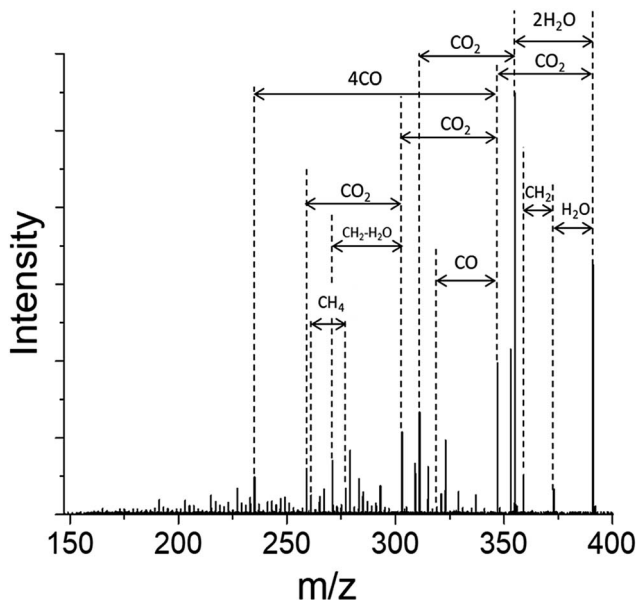
Fig. 3 A typical FT-ICR MS/MS spectrum from a 391 m/z precursor ion isolated at nominal mass and subjected to CID prior to injection in the ICR cell.

pathway and are not considered. For example, CO_2 can be associated with carboxyl groups and H_2O loss with the presence of hydroxyl groups. In addition, we observed the CO, CH_2, and CH_4 neutral losses (see Table S2† for all neutral loss fragments observed), in good agreement with previous FT-ICR MS/MS reports.[37] Taking advantage of the high mass accuracy of the FT-ICR MS measurements, neutral loss assignments can be easily identified. For example, the fragmentation pathways for 391.1031 m/z ($C_{19}H_{19}O_9$, Table S3†) were generated utilizing the fragmentation data obtained at nominal mass (Table S1†) and all possible combinations of neutral loss fragments (Table S2†) with a mass tolerance error of 1 mDa. Duplicate fragmentation pathways with the same syntaxes were eliminated (*e.g.*, $2CH_2$–$3CO$ is the same as $3CO$–$2CH_2$), since sequential fragmentation was not performed. Inspection of the fragmentation pathway shows a total of 16 end core fragments, each of them with multiple neutral loss pathways (see Table 1 and S3†). Since each pathway denotes the number and type of functional groups that were lost during fragmentation, the number of pathways could provide an upper estimate of the number of structural isomers. For instance, $3CO_2$–$2CO$–$2CH_4$ is one of the fragmentation pathways ending in the core formula $C_{12}H_{11}O$ (m/z 171.0814). That is, the parent ion ($C_{19}H_{19}O_9$, 391.1031) presumably experienced losses of three carboxylic groups, two carbonyl groups and two methane groups, suggesting that one isomer structure contains an arrangement of these functional groups. Conversely, for the same ending core formula ($C_{12}H_{11}O$), another fragmentation pathway involved consecutive losses of two hydroxyl groups, one carboxyl group, two methylene groups and four carbonyl groups ($2H_2O$–CO_2–$2CH_2$–$4CO$), indicating the presence of a different structural isomer.

Table 1 Core fragments and number of neutral loss pathways observed for 391.1031 m/z ($C_{19}H_{19}O_9$) during ESI-q-FT-ICR-MS/MS with isolation at nominal mass

Precursor ion m/z	Core fragment m/z	Structural isomers
391.1031 $C_{19}H_{19}O_9$	161.0607 $C_{10}H_9O_2$	13
	163.0763 $C_{10}H_{11}O_2$	7
	165.0192 $C_8H_5O_4$	3
	165.056 $C_9H_9O_3$	2
	167.0349 $C_8H_7O_4$	1
	171.0814 $C_{12}H_{11}O$	23
	173.0607 $C_{11}H_9O_2$	23
	175.0400 $C_{10}H_7O_3$	15
	183.0450 $C_{12}H_7O_2$	40
	183.0814 $C_{13}H_{11}O$	25
	185.0607 $C_{12}H_9O_2$	29
	187.0400 $C_{11}H_7O_3$	25
	201.0192 $C_{11}H_5O_4$	25
	202.9984 $C_{10}H_3O_5$	15
	205.0140 $C_{10}H_5O_5$	7
	241.0140 $C_{13}H_5O_5$	7

A parallel analysis performed using *in silico* fragmentation of 391.1031 m/z ($C_{19}H_{19}O_9$) with the MetFrag CL software across PubChem, that included the MS/MS information at nominal mass, resulted in 96 hits (see Fig. S1†). That is, 96 candidate structures were obtained based on the accurate mass of the precursor and fragment ions with 1 mDa mass tolerance.

While the ESI-q-FT-ICR MS/MS analysis with nominal mass quadrupole isolation is suggested as a rapid way to estimate an upper limit of the structural diversity and complexity of DOM, it is important to consider, that because the isolation was only performed at the level of nominal mass, potential over-estimation of the number of pathways is possible due to rearrangements of the fragments during CID. That is, interferences from fragments from other isobaric parent ions with similar chemical compositions (*i.e.*, $C_cH_hO_o$) may be a limitation in this approach (see Fig. 2). Nevertheless, the data summarized in Table 1 suggest the presence of up to 260 structural isomers. When compared to IMS data and MetFrag output, we can speculate that there are multiple structural isomers that share the same IMS band (only seven bands separated by the SAME algorithm).

Conclusions

In the present work, we illustrated the advantages of ESI-TIMS-FT-ICR MS/MS to address the isomeric content of DOM. The MS analysis permitted the identification of chemical components based on mass accuracy. When complemented with IMS measurements, an estimate of structural and conformational isomers can be obtained (*e.g.*, an average of 6–10 isomers were observed). While the MS spectra allowed the observation of a large number of peaks (*e.g.*, PAN-L: 5004 and PAN-S: 4660), over 4× features were observed in the IMS-MS domain (*e.g.*, PAN-L: 22 015 and PAN-S: 20 954). Assuming a total general formula of $C_xH_yN_{0-3}O_{0-19}S_{0-1}$, 3066 and 2830 for PAN-L and PAN-S chemical assignments were found in

a single infusion experiment, respectively. Most of the identified chemical compounds ($\sim$80%) corresponded to highly conjugated oxygen compounds (O_1–O_{20}). Moreover, when ESI-q-FT-ICR MS/MS is performed at the level of nominal mass, further estimation of the number of structural isomers is possible based on unique neutral loss fragmentation patterns and core fragments. The data provided shows that multiple structural isomers could have very closely related CCS, which will demand the use of ultrahigh resolution TIMS mobility scan functions in tandem with MS/MS. Future studies can further push the analytical boundaries of ESI-TIMS-FT-ICR MS by mobility selective ESI-TIMS-FT-ICR MS/MS, and applying the correlated harmonic excitation field (CHEF)[37] on the quadrupole 1 Da isolated parent ions.

Conflicts of interest

There are no conflicts to declare.

Acknowledgements

Notes and references

1 L. A. Kaplan and R. M. Cory, in *Stream Ecosystems in a Changing Climate*, ed. J. J. a. E. Stanley, Academic Press, 2016, pp. 241–320.

2 N. Hertkorn, M. Harir, B. Koch, B. Michalke and P. Schmitt-Kopplin, *Biogeosciences*, 2013, **10**, 1583–1624.

3 M. Zark, J. Christoffers and T. Dittmar, *Mar. Chem.*, 2017, **191**, 9–15.

4 N. Hertkorn, M. Harir, K. M. Cawley, P. Schmitt-Kopplin and R. Jaffé, 2016.

5 T. Dittmar and A. Stubbins, *Treatise on Geochemistry*, Elsevier, Oxford, 2nd edn, 2014, pp. 125–156.

6 R. Jaffé, Y. Yamashita, N. Maie, W. Cooper, T. Dittmar, W. Dodds, J. Jones, T. Myoshi, J. Ortiz-Zayas and D. Podgorski, *Geochim. Cosmochim. Acta*, 2012, **94**, 95–108.

7 M. Zark and T. Dittmar, *Nat. Commun.*, 2018, **9**, 3178.

8 P. E. Rossel, A. V. Vähätalo, M. Witt and T. Dittmar, *Org. Geochem.*, 2013, **60**, 62–71.

9 L. V. Tose, P. Benigni, D. Leyva, A. Sundberg, C. E. Ramírez, M. E. Ridgeway, M. A. Park, W. Romão, R. Jaffé and F. Fernandez-Lima, *Rapid Commun. Mass Spectrom.*, 2018, **32**, 1287–1295.

10 E. W. Robinson and E. R. Williams, *J. Am. Soc. Mass Spectrom.*, 2005, **16**, 1427–1437.

11 E. W. Robinson, D. E. Garcia, R. D. Leib and E. R. Williams, *Anal. Chem.*, 2006, **78**, 2190–2198.

12 E. W. Robinson, R. D. Leib and E. R. Williams, *J. Am. Soc. Mass Spectrom.*, 2006, **17**, 1470–1480.

13 E. W. Robinson, R. E. Sellon and E. R. Williams, *Int. J. Mass Spectrom.*, 2007, **259**, 87–95.

14 J. Saba, E. Bonneil, C. Pomiès, K. Eng and P. Thibault, *J. Proteome Res.*, 2009, **8**, 3355–3366.

15 Y. Xuan, A. J. Creese, J. A. Horner and H. J. Cooper, *Rapid Commun. Mass Spectrom.*, 2009, **23**, 1963–1969.

16 G. Bridon, E. Bonneil, T. Muratore-Schroeder, O. Caron-Lizotte and P. Thibault, *J. Proteome Res.*, 2012, **11**, 927–940.

17 W. Schrader, Y. Xuan and A. Gaspar, *Eur. J. Mass Spectrom.*, 2014, **20**, 43–49.

18 F. A. Fernandez-Lima, C. Becker, A. M. McKenna, R. P. Rodgers, A. G. Marshall and D. H. Russell, *Anal. Chem.*, 2009, **81**, 9941–9947.

19 M. Fasciotti, P. M. Lalli, C. F. Klitzke, Y. E. Corilo, M. A. Pudenzi, R. C. L. Pereira, W. Bastos, R. J. Daroda and M. N. Eberlin, *Energy Fuels*, 2013, **27**, 7277–7286.

20 P. Benigni, C. J. Thompson, M. E. Ridgeway, M. A. Park and F. Fernandez-Lima, *Anal. Chem.*, 2015, **87**, 4321–4325.

21 P. Benigni and F. Fernandez-Lima, *Anal. Chem.*, 2016, **88**, 7404–7412.

22 Y. Pu, M. E. Ridgeway, R. S. Glaskin, M. A. Park, C. E. Costello and C. Lin, *Anal. Chem.*, 2016, **88**, 3440–3443.

23 M. E. Ridgeway, J. J. Wolff, J. A. Silveira, C. Lin, C. E. Costello and M. A. Park, *Int. J. Ion Mobility Spectrom.*, 2016, **19**, 77–85.

24 P. Benigni, K. Sandoval, C. J. Thompson, M. E. Ridgeway, M. A. Park, P. Gardinali and F. Fernandez-Lima, *Environ. Sci. Technol.*, 2017, **51**, 5978–5988.

25 P. Benigni, R. Marin, K. Sandoval, P. Gardinali and F. Fernandez-Lima, *J. Visualized Exp.*, 2017, **121**, e55352.

26 P. Benigni, C. Bravo, J. M. E. Quirke, J. D. DeBord, A. M. Mebel and F. Fernandez-Lima, *Energy Fuels*, 2016, **30**, 10341–10347.

27 P. Benigni, J. Porter, M. E. Ridgeway, M. A. Park and F. Fernandez-Lima, *Anal. Chem.*, 2018, **90**, 2446–2450.

28 D. R. Hernandez, J. D. DeBord, M. E. Ridgeway, D. A. Kaplan, M. A. Park and F. Fernandez-Lima, *Analyst*, 2014, **139**, 1913–1921.

29 F. A. Fernandez-Lima, D. A. Kaplan and M. A. Park, *Rev. Sci. Instrum.*, 2011, **82**, 126106.

30 F. Fernandez-Lima, D. Kaplan, J. Suetering and M. Park, *Int. J. Ion Mobility Spectrom.*, 2011, **14**, 93–98.

31 E. R. Schenk, M. E. Ridgeway, M. A. Park, F. Leng and F. Fernandez-Lima, *Anal. Chem.*, 2014, **86**, 1210–1214.

32 E. R. Schenk, V. Mendez, J. T. Landrum, M. E. Ridgeway, M. A. Park and F. Fernandez-Lima, *Anal. Chem.*, 2014, **86**, 2019–2024.

33 E. W. McDaniel and E. A. Mason, *Mobility and diffusion of ions in gases*, John Wiley and Sons, Inc., New York, 1973.

34 P. Benigni, K. Sandoval, C. J. Thompson, M. E. Ridgeway, M. A. Park, P. Gardinali and F. Fernandez-Lima, *Environ. Sci. Technol.*, 2017, **51**, 5978–5988.

35 C. Ruttkies, E. L. Schymanski, S. Wolf, J. Hollender and S. Neumann, *J. Cheminf.*, 2016, **8**, 3.

36 A. Stubbins, R. G. M. Spencer, H. M. Chen, P. G. Hatcher, K. Mopper, P. J. Hernes, V. L. Mwamba, A. M. Mangangu, J. N. Wabakanghanzi and J. Six, *Limnol. Oceanogr.*, 2010, **55**, 1467–1477.

37 M. Witt, J. Fuchser and B. P. Koch, *Anal. Chem.*, 2009, **81**, 2688–2694.